



African Journal of Biological Sciences



Structural and Dispersion Parameters of PVA-PEG Blend Prepared via Electrospinning Technique with Various Additives of CaF₂ nanoparticles

¹Akeel Shakir Alkelaby, ¹Mohammad Taghi Ahmadi, ¹Asghar Esmaeili, ¹Hassan Sedghi, ²Khalid Haneen Abass.

¹Physics Department, Faculty of Science, Urmia University, Urmia, Iran

²Physics Department, College of Education for Pure Sciences, University of Babylon, Iraq.

Corresponding author: pure.khalid.haneen@uobabylon.edu.iq

Abstract

In this study, a novel nanofiber was fabricated using electrospinning. This nanofiber was composed of Poly (vinyl alcohol) (PVA) and polyethylene glycol (PEG), and was doped with different ratios (0.001, 0.002, 0.003) of CaF₂ at room temperature. Optical microscopy images demonstrated a fine and homogeneous dispersion of the nanomaterial within the samples. Scanning Electron Microscopy (SEM) analysis revealed a random distribution of fine fibers in both the polymer blend and doped samples. Prior to the addition of CaF₂, the average diameter of the nanofibers was 68.97 nm. Following the addition of CaF₂, the average diameters were measured to be 45.76 nm, 68.71 nm, and 98.45 nm for each respective sample. These fibers exhibited a smooth surface. As the concentration of the nanomaterial increased, the transmittance spectra decreased. Concurrently, the extinction coefficient increased with the increasing content of CaF₂. The values of the dielectric constant (real and imaginary) increased with increasing CaF₂ concentrations, and this is attributed to the increase in electrical polarization in the nanofibers due to the contribution of the concentration in the sample, i.e. the increase in charges within the polymers. The Wemple-DiDomenico model was used to derive the dispersion coefficients such as E_o, E_d, n_o, M₋₁, and M₋₃.

Keywords: PVA-PEG-CaF₂, nanofibers, Electrospinning, structural and Dispersion parameters.

Article History

Volume 6, Issue 5, 2024

Received: 22 May 2024

Accepted: 29 May 2024

doi:10.33472/AFJBS.6.5.2024.8372-8394

Introduction

Polymers have rapidly become an indispensable component of modern life, owing to their versatility, affordability, low operational expenses, ease of processing, and desirable chemical, physical, and optical properties [1]. A polymer is composed of numerous molecules, each consisting of thousands of atoms bonded together by covalent bonds. Furthermore, the molecules within a polymer are attracted to each other through various forces, which vary depending on the particular type of polymer [2]. Similar to conventional composites, a nanocomposite is comprised of a matrix and filler. However, nanocomposites employ nanoparticle fillers instead of the fiber fillers typically used in traditional composites, such as carbon or fiberglass [3]. Materials such as CNTs, carbon nanofibers, and other metal or semiconductor nanoparticles like silicon, gold, silver, diamond, and copper fall under this category of nanoparticle fillers [4]. Polymer nanofibers are an essential category of nanostructured materials, finding applications in various fields such as biology, electronics, healthcare, protective gear, and wastewater treatment. Recent advancements in manufacturing techniques, including phase separation, electrospinning, drawing, and template synthesis have streamlined production processes and expanded the range of possible applications [5].

The electrospinning technique is widely recognized for its simplicity, cost-effectiveness, flexibility, and efficiency in creating one-dimensional nanostructured materials. Among the various methods available for producing such materials at a low cost and with great flexibility, electrospinning stands out as particularly noteworthy [6]. PVA, short for polyvinyl alcohol, is gaining recognition as a highly promising polymer due to its impressive properties. These properties include excellent water solubility, high dielectric strength, chemical stability, and eco-friendliness. The presence of hydroxyl groups in PVA facilitates strong interconnections within polymer composites through hydrogen bonding [7]. Polyvinyl

alcohol, or PVA, finds extensive applications in various industries such as electronics, construction, medicine, and more. This widespread use can be attributed to the numerous advantages offered by this polymer[8]. Polyethylene glycol, or PEG, is a well-known polymer that is cherished for its accessibility, low cost, and safety[9]. Polyethylene glycols, or PEGs, are a class of polymers with a variety of characteristics that can be liquid or solid [10]. To enhance elasticity, various polymers can be incorporated for this purpose. The addition of plasticizers helps alleviate molecular rigidity by reducing the intermolecular forces along the polymer chain[11]. Calcium Fluoride (CaF_2) is an insoluble ionic compound consisting of Ca_2^+ and F^- ions. It occurs naturally in minerals like "Fluorite" (or fluorspar) and "Blue-John" and is a valuable global source of fluorine. Structurally, it adopts a cubic arrangement in which each calcium ion is surrounded by eight fluoride anions, while each fluoride ion is coordinated with four calcium ions[12]. The remarkable properties of CaF_2 , including its low refractive index, low phonon energy, stability over a broad visible spectrum (200–1100 nm), and large band gap of 12 eV, make it very attractive. Regardless of their doping condition, CaF_2 molecules are widely utilized in nanotechnology for a variety of applications, such as spectroscopic windows and components in color displays[13]. CaF_2 can be used as a laser medium by doping it with rare earth elements[14]. In addition, CaF_2 is widely recognized for its thermo luminescent (TL) properties when doped with different impurities. Notably, CaF_2 doped with manganese ($\text{CaF}_2:\text{Mn}$) serves as an excellent dosimeter, accurately measuring extremely high levels of radiation exposure. [15]. The objective of this work is to synthesize PVA-PEG- CaF_2 nanofibers by electrospinning and assess their optical and dispersion parameters to candidate it in communication and optical devices.

Experimental

Materials

The experiment utilized two polymers: PVA, procured from the DIDACTIC company, with a molecular weight of 18000 and a purity of 99%, and PEG, obtained from Reagent World, with a molecular weight of 600 and a purity of 99.8%. Both polymers exhibited granular morphology. Additionally, various quantities of CaF₂ nanoparticles with a purity of 90% were incorporated into the mixture.

preparation of PVA-PEG-CaF₂ nanofibers

Two grams of polymer (PVA-PEG-CaF₂) nanofibers were prepared in the following manner: 1.6 grams of PVA powder were dissolved in 60 milliliters of distilled water using a glass beaker equipped with a magnetic stirrer. The mixing process continued for 45 minutes at a temperature of 90°C to ensure a more uniform solution. Subsequently, PEG weighing 0.4 grams was added to the mixture in intermittent doses, and the mixture was left for another 45 minutes to attain a suitably thick liquid consistency at 90°C. Constant stirring was maintained until homogeneity was achieved. Following this, three additions of CaF₂ (0.001, 0.002, and 0.003 grams) were introduced to the mixture, with each addition being dispersed by using a two-minute ultrasonication process. Each addition of CaF₂ was allowed to mix for 45 minutes to ensure proper dispersion. The resulting mixture was then used for electrospinning to prepare (PVA-PEG) nanofibers with varying amounts of CaF₂ additives, as indicated in Table (1).

Table 1. Weight of PVA-PEG- CaF₂nanofiber

PVA	PEG	CaF ₂
(g)	(g)	(g)

1.6	0.4	0.0
1.6	0.4	0.001
1.6	0.4	0.002
1.6	0.4	0.003

Electrospinning process

In this study, a horizontal electrospinning setup was utilized. This involved placing the syringe pump in a horizontal position. After completing the solution mixing process, the prepared solutions were loaded into standard 2 mL syringes that were attached to stainless steel needles, serving as jets. The needle-jets were horizontally positioned in front of a metal collector. In the electrospinning process, the tip of the needle jet was connected to the positive electrode, while the metal collector was connected to the negative electrode. To serve as a target for nanofiber deposition, aluminum foil was utilized to cover the metal collector.

The electrospinning process was conducted at room temperature. The spinning parameters required for fabricating the specimens are detailed in Table(2).

Table 2. Electrospinning parameters used to fabricating specimens.

Electrospinning parameters	Specification
Applied voltage	23 kV
Orifice size	0.7 mm
Collector distance	10 cm
Rotation speed	500 rpm
Flow rate	0.5 ml/hr
Temperature	25 °C

Results and Discussions

SEM was employed to analyze the surface morphology of the samples and assess the dispersion of CaF₂ within the polymer matrix. Figure 2 depicts SEM images of both the PVA-PEG polymer blend and PVA-PEG:CaF₂ nanofibers, exhibiting different amounts of CaF₂ (0. g, 0.002 g, and 0.003 g) at magnifications of 110,000x and 50,000x. Prior to the addition of CaF₂, the fibers exhibited an average diameter of 68.97 nm. After the incorporation of CaF₂ in each sample, the average diameter of the nanofibers ranged from 45.76 to 98.45 nm, as determined using software analysis (ImageJ). The nanofibers exhibit a smooth surface. In contrast, the microfibers appear to form randomly, with intersections frequently occurring among the nanofibers. The entanglement of chains is deemed a vital feature for maintaining the stability of the liquid jet throughout the electrospinning process [16]. During the electrospinning process, different morphologies of fibers and/or beads can be produced due to specific combinations of solution properties and experimental settings. Variables that can be controlled to produce different structures are related to the polymer (such as molecular weight, polydispersity index, T_g, isomeric structure, and crosslinking). They may also be related to the solution (including type of solvent, concentration, viscosity, electrical conductivity, dielectric strength, surface tension, additives, and temperature) or the process (such as applied field intensity, deposition distance, flow rate, deposition time, solvent evaporation rate, capillary size, collection technique, and relative humidity)[17]. The effects of various parameters on the morphology of the electrospun polymer can be summarized in the following figure 1 [18]. Generally, the concentration of the polymer solution is a critical factor in determining fiber formation during the electrospinning process. If the concentration is too low, the solution will have low viscosity and high surface tension. This can lead to the formation of polymeric micro

(nano)-particles through electrospray, rather than through electrospinning[19]. Alternatively, when the concentration is marginally increased, a composite of beads and fibers is produced. However, when the concentration reaches an optimal level, the formation of smooth nanofibers is achieved[20]. Viscosity is a critical factor in shaping the morphology of electrospun fibers. Insufficient viscosity can impede the creation of continuous and smooth fibers. Conversely, an overly high viscosity can pose challenges for the jet to be expelled from the solution. Hence, attaining a suitable viscosity is vital for successful electrospinning[21,22]. Surface tension, which is influenced by the solvent composition of the solution, is another important factor in electrospinning [23]. It has been established that the mean diameter of electrospun nanofibers bears a direct correlation with the solution's shear viscosity. As the average viscosity of the solution escalates, nanofibers with larger diameters are typically produced[24]. The relationship is outlined in Equation (1). In a nutshell, the concentration and viscosity of the polymer solution, together with the surface tension, are key parameters that have a significant influence on the morphology and diameter of the electrospun nanofibers. Determining the right equilibrium among these factors is crucial for producing the desired fiber properties in electrospinning.

$$d \sim \eta \lambda \dots\dots\dots(1)$$

Equation (1) describes the relationship between the average diameter of electrospun fibers (d), the shear viscosity of the solution (η), and the yield exponent (λ). The value of the yield exponent (λ) is typically greater than 1/3 for the scaling law, although it may vary for different polymer solutions [25]. For successful electrospinning, it is essential to keep both the voltage and viscosity of the polymer solution within a certain range. Elements such as the concentration of the solution, flow rate, working distance, and the voltage of the electrospinning platform collectively contribute to the

creation of continuous fibers with uniform shape and minimal beading. However, an overly high concentration of the solution can adversely impact the production of nanofibers due to unsuitable solution viscosity, which obstructs the formation of fibers[26].





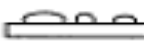

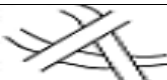
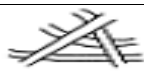

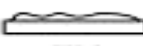

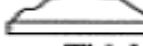
Parameter	Normalized Magnitude		
	Low	Average	High
Solution Concentration top view	 Beads		 Filaments
Deposition Distance side view	 Flat		 Round
Applied Field Strength top view	 Wide		 Narrow
Deposition Time side view	 Thin		 Thick

Figure 1. Schematic illustration of the effects of process parameters on the the structure of the electrospun product [18].

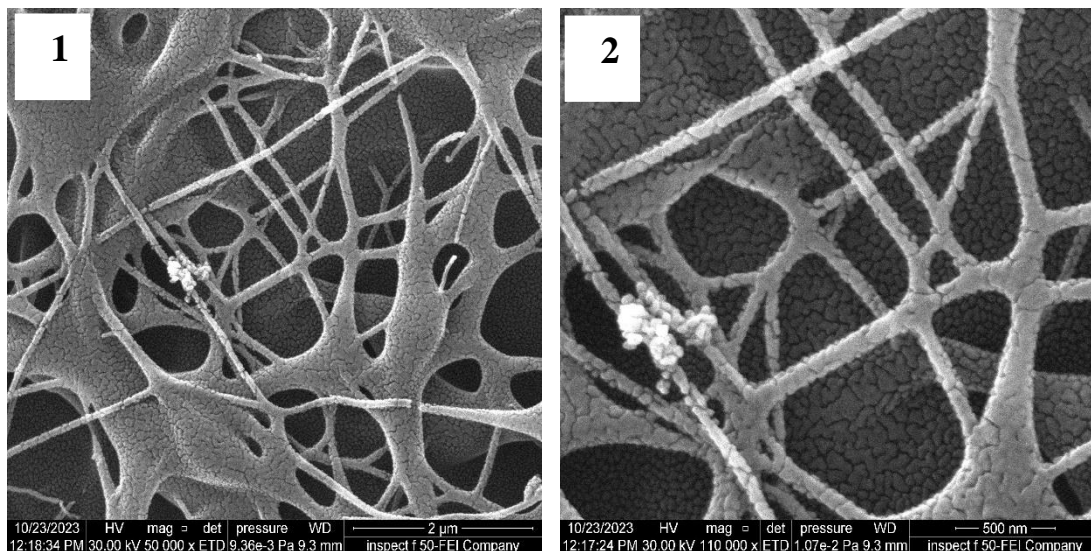


Figure (2 A): SEM images of PVA- PEG of nanofibers with varying magnifications: (1) 50 kx and (2) 110 kx.

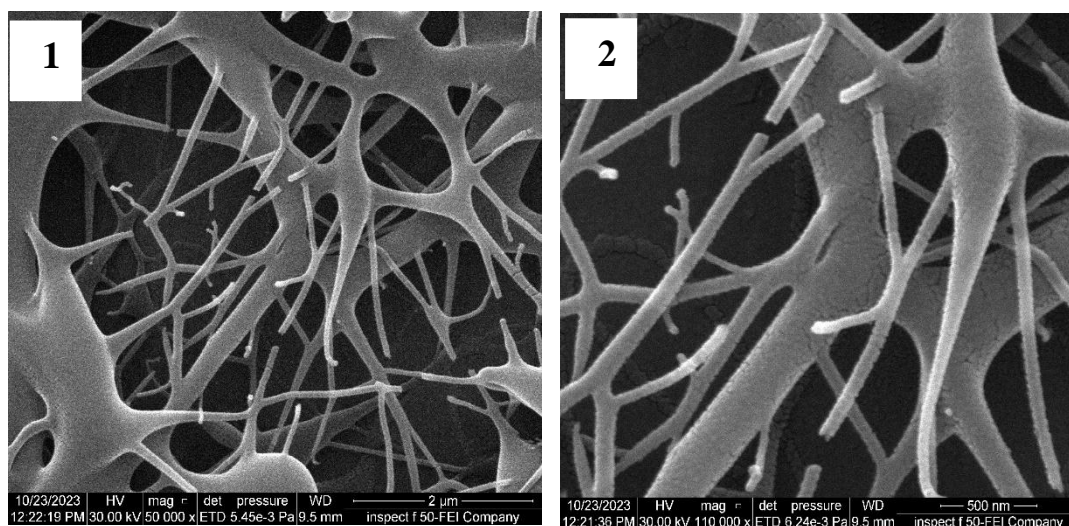


Figure (2 B): SEM of electrospun PVA-PEG images of nanofibers with add 0.001ml CaF₂ taken at varying magnifications: (1) 50kx and (2) 110 kx.

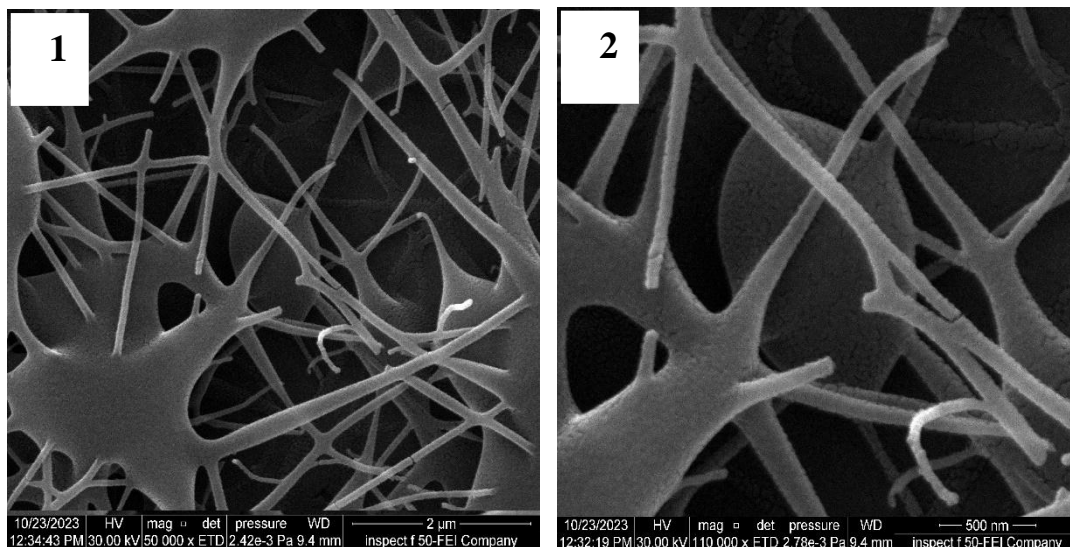


Figure (2 C): SEM of electrospun PVA-PEG images of nanofibers with add 0.002ml CaF₂ taken at varying magnifications: (1) 50kx and (2) 110 kx.

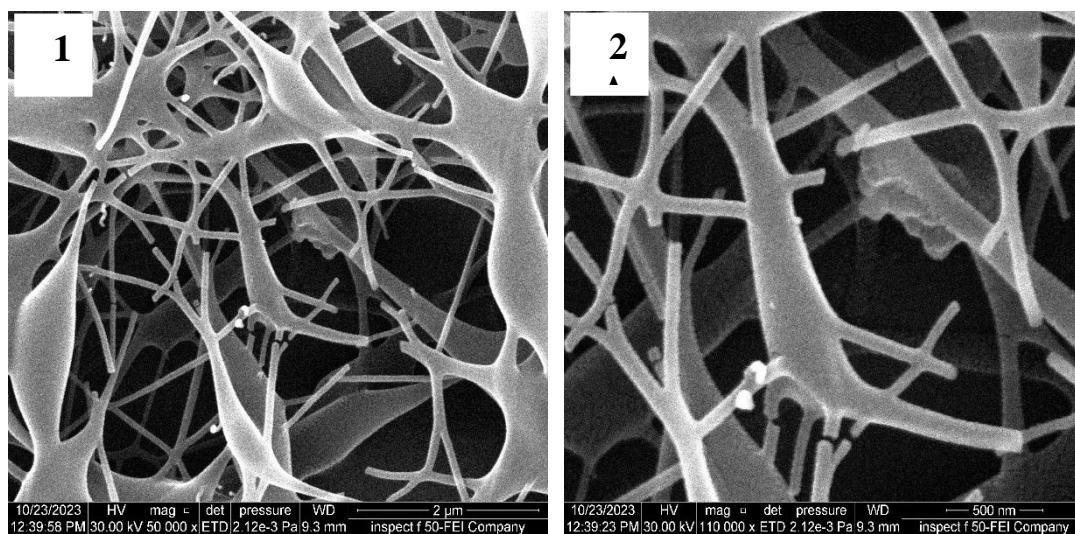


Figure (2D): SEM of electrospun PVA-PEG images of nanofibers with add 0.003ml CaF₂ taken at varying magnifications: (1) 50kx and (2) 110 kx.

The OM images verify the successful fabrication of PVA-PEG-CaF₂ nanofibers using the casting method. These images expose a uniform matrix with CaF₂ evenly distributed throughout the polymer blend composites. In particular, Figure 3-a displays the PAAm-PEG blend, signifying the effective dissolution of the polymers.

Parts (b, c, and d) of Figure 3 illustrate the diffusion of CaF₂ within the PAAm-PEG blend, revealing a well-dispersed distribution of nanoparticles within the blend.

Notably, no aggregation of nanoparticle is observed that is related to the interaction among polymers and CaF₂ facilitated by the high surface-to-volume ratio. At a high concentration of CaF₂ nanofibers, specifically at a weight of 0.003, a continuous network of paths forms, enabling charge carriers to traverse. This leads to a modification of the material properties[27].

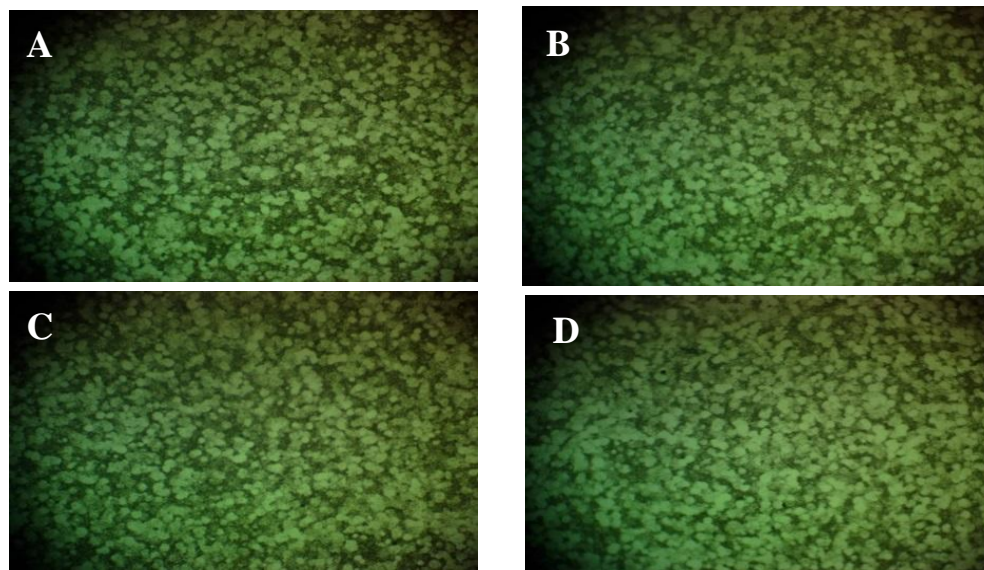


Figure 6. Photomicrographs (100X) of (PVA- PEG) with various content of CaF₂: (A) 0 CaF₂ (B) 0.001 CaF₂ (C) 0.002 CaF₂ and (D) 0.003 CaF₂.

The transmittance spectra (T) was calculated by[28]:

$$T = I_T/I_0 \quad (2)$$

Where I_T is the intensity of transmitted rays from the film and I_0 intensity of incident rays on the film.

Figure 4 presents the transmittance spectra (T) of PVA-PEG-CaF₂ nanofibers, demonstrating varying concentrations of CaF₂ across different wavelengths. Unlike absorbance spectra, transmittance spectra decrease with an increase in CaF₂ concentrations. This decrease is attributed to the presence of CaF₂, which harbors electrons capable of absorbing electromagnetic energy and transitioning to higher energy levels. Conversely, the pure sample displays high transmittance due to the absence of particles. In this scenario, there are no free electrons, thus requiring high energy for transitions and bond breakage[29].

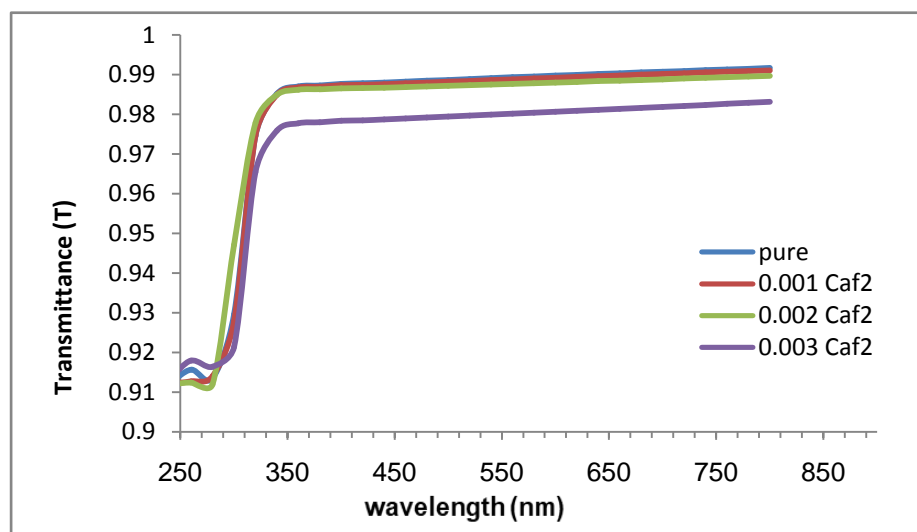


Figure 7. The transmittance versus wavelength of PVA-PEG-CaF₂ nanofiber with various content of CaF₂.

Studying the performance of the extinction coefficient (k_0) is crucial as it plays a significant role in determining the optical properties of materials[30]. The extinction coefficient (k_0) was calculated by[31]:

$$k_0 = \alpha\lambda/4\pi \quad \dots\dots\dots (3)$$

Figure 5 depicts the variation in the extinction coefficient (k_0) for PVA-PEG-CaF₂ nanofibers across a range of wavelengths. It shows a marked increase with higher concentrations of CaF₂. This trend can be ascribed to the enhanced optical absorption and photon dispersion within the PVA-PEG polymer blend as the concentration of CaF₂ increases. Notably, the extinction coefficient exhibits higher values in the UV region, which is primarily due to the significant absorbance of the nanofiber samples within this range. Consequently, the extinction coefficient of the nanofibers is particularly pronounced at UV wavelengths. Although the absorption coefficient of the nanofibers remains relatively stable from the visible to the near-infrared spectrum, the extinction coefficient shows an upward trend with increasing wavelengths[32].

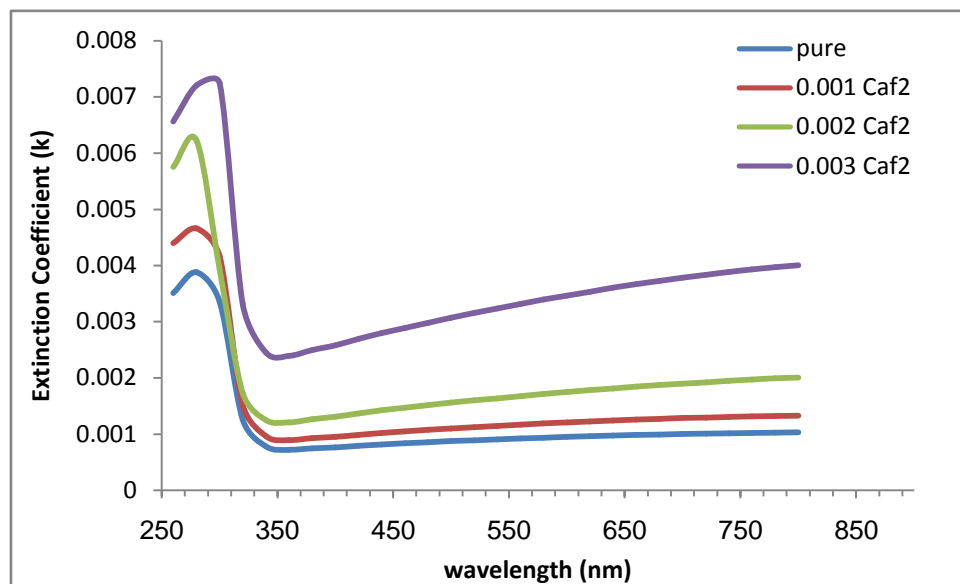


Figure 8.The Extinction coefficient versus wavelength of PVA-PEG-CaF₂ nanofiber with various content of CaF₂.

Dielectric constants offer valuable insights into the electronic band structure of materials. The rate of decrease in light velocity within a material is linked to the real component of the dielectric constant (ϵ_1). Meanwhile, the imaginary component of the dielectric constant (ϵ_2) serves as a fundamental optical parameter, correlating with the refractive index

and the extinction coefficient. The calculation of the dielectric constant for both components (ϵ_1 and ϵ_2) involved [33]:

$$\epsilon_1 = n^2 - k_0^2 \dots \dots \dots (4)$$

$$\epsilon_2 = 2n k_0 \dots \dots \dots (5)$$

Figures 6 and 7 illustrate the variations in the real and imaginary components of the dielectric constant for PVA-PEG-CaF₂ nanofibers across different wavelengths and concentrations of CaF₂. It's clear that both components of the dielectric constant increase with the rise in CaF₂ concentration. This trend can be attributed to the increased electrical polarization within the nanofibers, which is a result of the higher CaF₂ concentration in the sample. As a consequence, there is a proportional increase in charges within the polymers that make up both the PVA-PEG blends and the PVA-PEG-CaF₂ nanofibers.

Additionally, the figures display variations in both the real and imaginary components of the dielectric constant across different wavelengths. This behavior is primarily due to the real component of the dielectric constant's dependence on the refractive index, with little influence from the extinction coefficient. Conversely, the imaginary component of the dielectric constant is impacted by the extinction coefficient, particularly in the visible and near-infrared regions. In these regions, the refractive index remains relatively constant, while the extinction coefficient increases with wavelength[34,35].

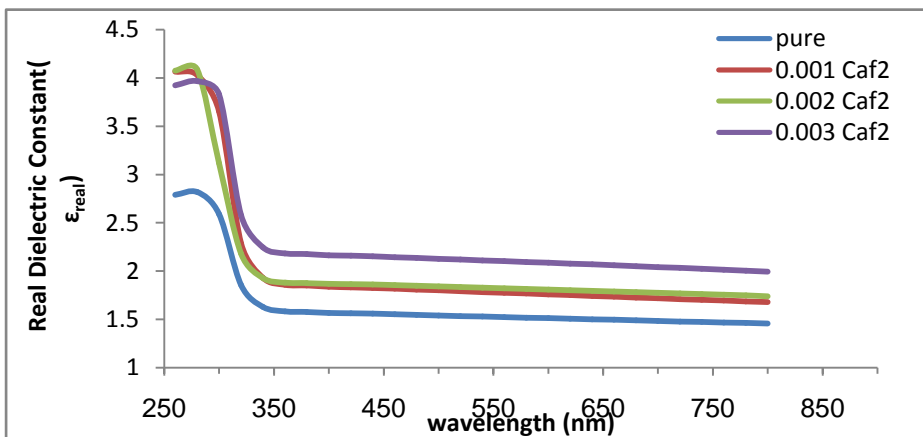


Figure 9. The real dielectric constant with the wavelength of PVA-PEG-CaF₂ nanofiber with various content of CaF₂.

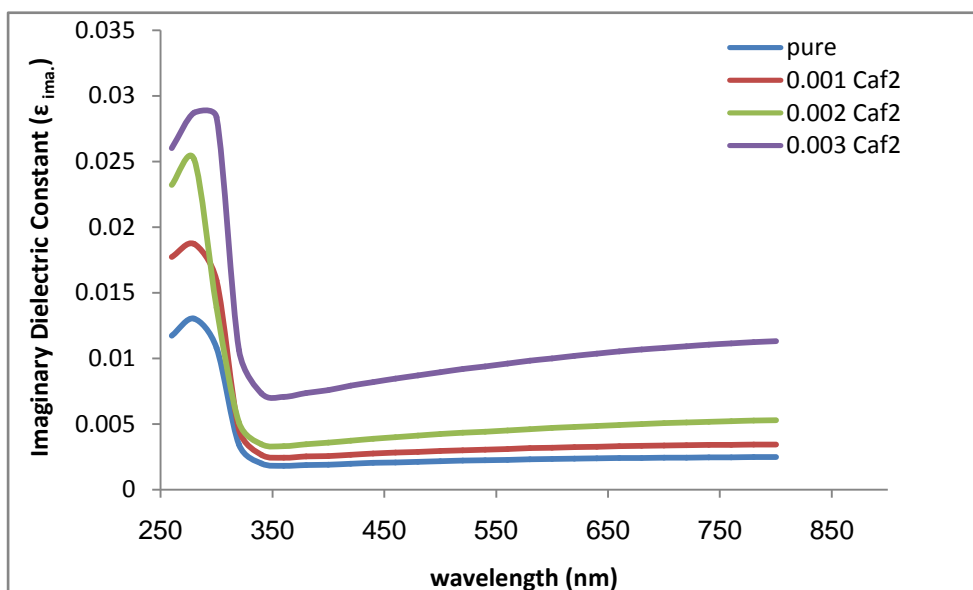


Figure 10. The Imaginary Dielectric Constant with the Wavelength of PVA-PEG-CaF₂ nanofiber with various content of CaF₂.

3.1 Dispersion Parameters

The refractive index dispersion data in materials has been analyzed using the concept of the single-oscillator. Within this concept, the energy parameters E_d and E_0 are introduced and the refractive index n at a photon energy ($h\nu$) can be expressed by Wemple and DiDomenico model for (PVA-PEG) blends and PVA-PEG -CaF₂) nanofibers. From the

equations (6-10) the values E_0 , E_d , E_g , n_0 , ϵ_∞ , M_{-1} and M_{-3} were calculated [36,37].

$$(n^2 - 1) = \frac{E_d E_0}{E_0^2 - (h\nu)^2} \quad (6)$$

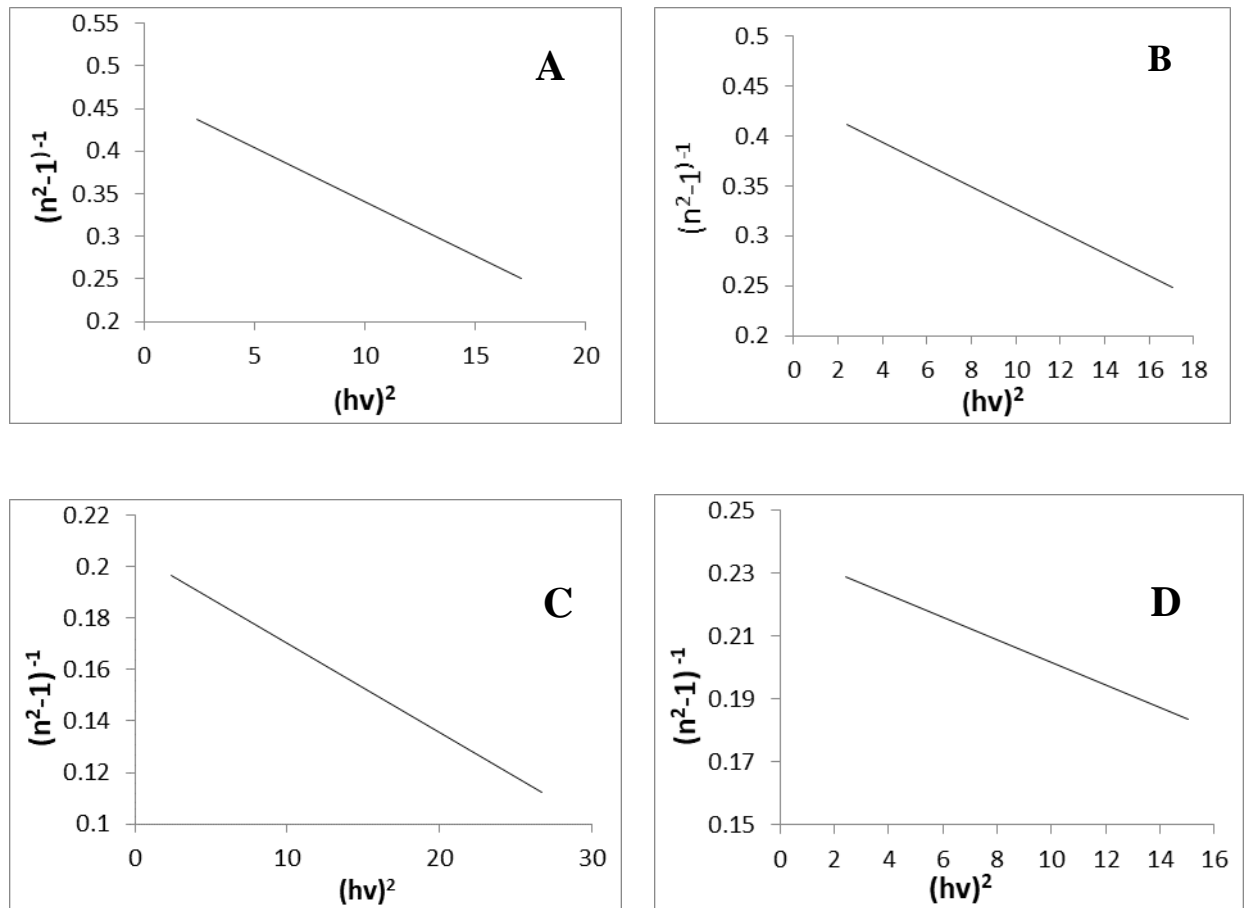
$$n_0^2 = 1 + \frac{E_d}{E_0} \quad (7)$$

$$\epsilon_\infty = n_0^2 \quad (8)$$

$$E_0^2 = \frac{M_{-1}}{M_{-3}} \quad (9)$$

$$E_d^2 = \frac{M_{-1}^3}{M_{-3}} \quad (10)$$

From the graphic representation of the relationship between $(n^2 - 1) - 1$ and $(h\nu)^2$ in Figure (8) used the slope $(E_0 E_d)^{-1}$ and the intercept $(\frac{E_0}{E_d})$ to determine E_0 and E_d . It calculated values were reported in Table (3), which demonstrated a decline in their values when $(CaF_2)NPs$ concentrations increased, the oscillator strength (E_0) and the dispersion energy linked with the energy of optical transitions (E_d) are shown to decrease as $(CaF_2)NPs$ increases, but the other parameters n_0 , ϵ_∞ , M_{-1} and M_{-3} increase, this phenomenon can be attributed to the shift of the optical transmission spectra towards longer wavelengths, which corresponds to the shift of the absorption edge towards shorter energy wavelengths. The calculated optical energy gap (the approximation relation $E_0 \approx 2E_g$) using the Tauc relation and the Wemple-DiDomenico estimate both had similar values. The findings concur with those of earlier researchers [38-41].



**Figure(8): Plot of $(n^2 - 1)^{-1}$ vs $(hv)^2$ of PVA-PEG with various content of CaF_2 :
(A) 0 CaF_2 (B) 0.001 CaF_2 (C) 0.002 CaF_2 and (D) 0.003 CaF_2 .**

Table (3): Optical parameters of PVA-PEG- CaF_2 nanofiber.

parameter	PVA--PEG			
	0 wt.	0.001wt. CaF_2	0.002wt. CaF_2	0.003wt. CaF_2
E_o^2	36.15384615	40.33333333	61.38461538	66.90909091
E_o	6.012806845	6.350852961	7.834833462	8.17979773
E_g	3.006403422	3.175426481	3.917416731	4.089898865
E_d	12.79320605	14.43375673	37.30873077	34.08249054
$n^2(0)$	3.127659574	3.272727273	5.761904762	5.166666667
$n_o(0)$	1.768519034	1.809068067	2.400396793	2.273030283
ϵ	3.127659574	3.272727273	5.761904762	5.166666667
M_{-1}	2.127659574	2.272727273	4.761904762	4.166666667
M_{-3}	0.058850158	0.05634861	0.07757489	0.062273551

Conclusions

PVA-PEG-CaF₂ nanofibers were successfully produced by optimizing electrospinning parameters. These parameters included the composition of the spinning solution, the applied voltage, the spinning distance, and the flow rate. The fibers exhibited a mean average diameter of 68.97 nm prior to the addition of CaF₂. After the incorporation of CaF₂, the mean average diameter of each sample ranged from 45.76 nm to 98.45 nm. Scanning electron microscopy revealed that these fibers had a smooth surface. Furthermore, optical microscopy images demonstrated the fine and homogeneous dispersion of the nanomaterial within the samples. The transmittance spectra, which are inversely related to absorption, decrease as the concentration of the nanomaterial increases. Additionally, the extinction coefficient escalates with the increasing content of CaF₂. The values of dielectric constant (real and imaginary) increased with the increasing of CaF₂ concentrations, this attributed to the increase of electrical polarization in nanofibers due to contribution of concentration in the sample i.e., a increase in charges within the polymers. The Wemple-DiDomenico model was used to derive dispersion parameters such as E_o , E_d , n_o , M_{-1} , M_{-3} . The results of the dispersion parameters give information to fabricate the optical devices.

References

- [1] R. M. Radwan (2007), "Electron induced modifications in the optical properties of polypropylene," *J. Phys. D. Appl. Phys.*,40,2,374–379.
- [2] S.M.Al Asadi, F.J Hamood, K.H.Abass, S.K.Mohammed, I.M. Hassan, D.M.A. Latif, (2019), "The effect of MgO nanoparticles on structure and optical properties of PVAPAAm blend", *Research Journal of Pharmacy and Technology*, 12(6), 2768-2771.
- [3] J. Robertson (2004), "Realistic applications of CNTs", *Materials Today*,7,46-52.
- [4]. Devangamath SS, Lobo B, Masti SP, et al. (2020) Thermal, mechanical, and AC electrical studies of PVA–PEG–Ag₂S polymer hybrid material. *J Mater Sci Mater Electron* 31: 2904–2917.
- [5] V.Beachley, and X.Wen,(2010),"Structures: fabrication, biofunctionalization, and cell interactions", *Prog. Polym. Sci.*, 35, 868.
- [6] K. A. Shenoy (2008), "Effects of Multi-Wall Carbon Nanotubes on The Mechanical Properties of Polymeric Nanocomposites", M.Sc. Thesis, Department of Mechanical Engineering and the Faculty of the Graduate School of Wichita State University.
- [7] B. Ben Doudou, A. Vivet, J. Chen, A. Laachachi, T. Falher, and C. Poilâne (2014), "Hybrid carbon nanotube—silica/polyvinyl alcohol nanocomposites films: preparation and characterisation," *J. Polym. Res.*,21,4,1–9.
- [8] K.H.Abass and H.A. Hamed (2020), "Reduction of Energy Gap in ZrO₂ Nanoparticles on Structural and Optical Properties of Casted PVA–PAAm Blend", *Journal of Green Engineering*,10, 7,4166–4176.
- [9] A. Zied, B.M. Hussein, M.A. Asiri, A.M. (2015). "Characterization, in situ electrical conductivity and thermal behavior of immobilized PEG on MCM-41". *International Journal of Electrochemical Science*,10(6): 4873-4887.

- [10] B. W. Chieng, N. A. Ibrahim, W. M. W. Yunus and M. Z. Hussein (2014), "Poly(lactic acid)/Poly(ethylene glycol) Polymer Nanocomposites: Effects of Graphene Nanoplatelets", *Polymers*, 6, 93-104.
- [11] K. Nadarajah, (2005), "Development and characterization of antimicrobial edible films from crawfish chitosan" Dissertation, Louisiana State University Agricultural and Mechanical College, 18–22.
- [12] J. Hashim, K.H. Abass (2024). "Novel Preparation of $\text{Cu}_2\text{O}/\text{CaF}_2$ Nanofilms via Thermal Evaporation Technique: Effect of Thickness on its Energies". *Journal of Nanostructures*.
- [13] A. Bensalaha, M. Mortiera, G. Patriarcheb, P. Gredinc, and D. Viviena (2006), "Synthesis and optical characterizations of undoped and rare-earth-doped CaF_2 nanoparticles," *Journal of Solid State Chemistry*, 179, 8, 2636–2644.
- [14] M. Zahedifar and E. Sadeghi (2020), "Synthesis and dosimetric properties of the novel thermoluminescent $\text{CaF}_2:\text{Tm}$ nanoparticles," *Radiation Physics and Chemistry*, 81, 12, 1856–1861.
- [15] B.C. Hong and K. Kawano (2006), "Luminescence studies of the rare earth ions-doped CaF_2 and MgF_2 films for wavelength conversion," *Journal of Alloys and Compounds*, 408–412, 838–841.
- [16] Silva M. A., Crawford A., Mundy J., Martins A., J. V., Araújo P. V., Hatton R. L and Neves N. M "Evaluation of extracellular matrix formation in polycaprolactone and starch-compounded polycaprolactone nanofiber meshes when seeded with bovine articular chondrocytes", *Tissue Engineering Part A*, 15(2), 377-385, (2009).

- [17] Y.M Shin, M. M. Hohman, M. P. Brenner, GC Rutledge, 'Experimental characterization of electrospinning: the electrically forced jet and instabilities', *Polymer* 42. 9955-9967. (2001).
- [18] H. Fong, W. Liu, C. Wang, R. A, "Continuous yarns from electrospun fibers" *Polymer* 43. 775-780. (2002).
- [19] Review Carbon fibers for composites. *J Mater Sci* 35(6):1303–1313.(2000)
- [20]. MM. Bergshoef, GJ Vancso, "Continuous yarns from electrospun fibers" *Transparent nanocomposites with ultrathin, electrospun nylon-4, 6 fiber reinforcement. Adv Mater* 11(16):1362–1365. (1999)
- [21] Han SO, Son WK, Youk JH, Park WH (2008) Electrospinning of ultrafine cellulose fibers and fabrication of poly (butylene succinate) biocomposites reinforced by them. *J Appl Polym Sci* 107(3):1954–1959. doi:10.1002/app.26643 130 4 Applications of Electrospun Nanofibers.
- [22] C.Tang, H.Liu,"Cellulose nanofiber reinforced poly (vinyl alcohol) composite film with high visible light transmittance. *Compos Part A: Appl Sci Manuf*", *compositesa*, 39(10):1638–1643. (2008)
- [23]. H.Fong,"(Electrospun nylon 6 nanofiber reinforced BIS-GMA/TEGDMA dental restorative composite resins)",*Journal Polymer*, 45(7):2427–2432,(2004).
- [24] D. W. Schubert, *Macromol., Theory Simul.* 28, 1900006.
- [25] Q. Wang et al "Electrospun γ -Fe₂O₃ nanofibers as bioelectrochemical sensors for simultaneous determination of small biomolecules," *Anal. Chim.*,125–132, (2018).
- [26] Y. T. Jia, J. Gong, X. H. Gu, H. Y. Kim, J. Dong,X. YShen: *Carbohyd, journalPolym.* 67,403-409.(2007).
- [27] M.H Rasheed, F.S.Hashim, K.H Abass, "Impact of Ag Nanoparticles on the Spectral and Optical Properties of Electrospun Nanofibrous

- Poly(vinyl alcohol)-Poly(acrylamide)", *International Journal of Nanoscience*,22,3,(2023).
- [28] M. T. Ramesan, M. Varghese, P. Jayakrishnan, P. Periyat“Silver-Doped Zinc Oxide as a Nanofiller for Development of Poly(vinyl alcohol)/Poly(vinyl pyrrolidone), Blend Nanocomposites,” *Advances in Polymer Technology*,00,0,21650-7.(2016),
- [29] M. A.Da Silva, Crawford A., Mundy J., A.Martins, J. V. Araújo,P. V Hatton, R. L,Reis and N. M.Neves,“Evaluation of extracellular matrix formation in polycaprolactone and starch-compounded polycaprolactone nanofiber meshes when seeded with bovine articular chondrocytes”, *Tissue Engineering Part A*, 15(2), 377-385.(2009).
- [30]A. Badawi, S.J. Alsufyani, S.S. Alharthi, M.G. Althobaiti, A.A. Alkathiri, M. Almurayshid and A.NAlharbi, "Impact of gamma irradiation on the structural, linear and nonlinear optical properties of lead oxide incorporated PVA/graphene blend for shielding applications", *j. Opt. Mater.*,127 ,112244, (2022).
- [31] K.H.Abass andO.Haidar,"0.006wt.% Ag-Doped Sb₂O₃ Nanofilms with Various Thickness: Morphological and optical properties", *Journal of Physics: Conference Series*, 1294(2),(2019).
- [32] Reem Sami Ali, Noor Al-Huda Al-Aaraji, Esraa H. Hadi, Khalid HaneenAbass, Nadir Fadhil abubi, Sami Salman Chiad, "Effect of Lithium on Structural and Optical Properties of Nanostructured CuS ThinFilms", *J Nanostruct* 10(4): 810-816, 2020. DOI: 10.22052/JNS.2020.04.014.
- [33] A.S.Alkelaby, K.H.Abass, T.H.Mubarak, N.F. Habubi, S.S.Chiad, I.Al-Baidhany, "Effect of MnCl₂ additive on optical and dispersion parameters of poly methyl methacrylate films", *Journal of Global Pharma Technology* 11(4),347-352,(2019).
- [34] R. G. Kadhim“Study of Some Optical Properties of Polystyrene-Copper Nanocomposite Films”, *World Scientific News*,30,14.(2016).

- [35] J. Jose, M. A. Al-Harthi, M. A.-A. AlMa'adeed, J. B. Dakua, and S. K. De "Effect of graphene loading on thermomechanical properties of poly (vinyl alcohol)/starch blend," *Journal of Applied Polymer Science*, 132, 16, 2015. (2015).
- [36] A.F. Al-Shawabkeh, Z.M. Elimat and K.N. Abushgair "Effect of non-annealed and annealed ZnO on the optical properties of PVC/ZnO nanocomposite films" *J. Thermoplast. Compos. Mater.* 36 899–915.(2023)
- [37] K.S.Sharba, A.S.Alkelaby, M.D.Sakhil, K.H.Abass, N.F.Habubi, S.S.Chiad "Enhancement of urbach energy and dispersion parameters of polyvinyl alcohol with Kaolin additive". *NeuroQuantology*; 18(3): 66-73.(2020).
- [38] A.A.K. Zbala, A.O. Mousa Al-Ogaili and K.H.Abass, "Optical Properties and Dispersion Parameters of PAAm-PEG Polymer Blend Doped with Antimony (III) Oxide Nanoparticles" *NeuroQuantology* 20, 2, 62–68.(2022).
- [39] K.H., Abass, D.M.A.Latif, "The urbach energy and dispersion parameters dependence of substrate temperature of CdO thin films prepared by chemical spray pyrolysis", *International Journal of ChemTech Research*, 9(9),332-338,(2016).
- [40] S.H. Wemple and M.DiDomenico, "Behavior of the electronic dielectric constant in covalent and ionic materials" *Phys. Rev. B.* 3,4.(1971).
- [41] H.R.A.Mohammed, A.O.M. Al-Ogaili, K.H. Abass, "Structural and dispersion parameters of nano-layers prepared from Al-Ni-Cr alloy", *Materials Today: Proceedings*, 80, 2396-3304.(2023),